Using serosurveys to optimize surveillance for zoonotic pathogens

E. Clancey[1,*] **S.L. Nuismer**[2] **S.N. Seifert**[1]
[1]Paul G. Allen School for Global Health, Washington State University, Pullman, WA 99164 USA
[2]Department of Biological Sciences, University of Idaho, Moscow, ID 83844 USA
[*]Correspondence: erin.clancey@wsu.edu

ABSTRACT

Zoonotic pathogens pose a significant risk to human health, with spillover into human populations contributing to chronic disease, sporadic epidemics, and occasional pandemics. Despite the widely recognized burden of zoonotic spillover, our ability to identify which animal populations serve as primary reservoirs for these pathogens remains incomplete. This challenge is compounded when prevalence reaches detectable levels only at specific times of year. In these cases, statistical models designed to predict the timing of peak prevalence could guide field sampling for active infections. Here we develop a general model that leverages routinely collected serosurveillance data to optimize sampling for elusive pathogens. Using simulated data sets we show that our methodology reliably identifies times when pathogen prevalence is expected to peak. We then apply our method to two putative *Ebolavirus* reservoirs, straw-colored fruit bats (*Eidolon helvum*) and hammer-headed bats (*Hypsignathus monstrosus*) to predict when these species should be sampled to maximize the probability of detecting active infections. In addition to guiding future sampling of these species, our method yields predictions for the times of year that are most likely to produce future spillover events. The generality and simplicity of our methodology make it broadly applicable to a wide range of putative reservoir species where seasonal patterns of birth lead to predictable, but potentially short-lived, pulses of pathogen prevalence.

INTRODUCTION

Spillover of zoonotic pathogens is a pervasive challenge[1], imposing a persistent burden on human health and creating conditions ripe for the emergence of novel infectious disease[2]. One avenue to controlling the health impacts of spillover is to increase surveillance within the human population, treating disease as it occurs and using public health measures to keep initial events from expanding into epidemics or pandemics[3–5]. However, when surveillance and intervention systems fail, the results can be catastrophic (e.g., West African Ebola epidemic; COVID-19 pandemic).

An alternative approach to managing the risk of spillover is preemptive, and focuses on stopping spillover before it occurs. For instance, the risk of spillover could be managed by altering habitat availability for reservoir species[6,7], changing human behavior to reduce contact with hosts[8,9], or vaccinating reservoir species[10,11]. For these preemptive approaches to work, we must know which animal species serve as important reservoirs for a pathogen of interest. Recent progress in this direction has been made by capitalizing on advances in machine learning that allow models to learn which suites of traits are associated with suitability as a reservoir[2,12]. For instance, Schmidt et al.[13] used boosted regression trees to predict which species are most likely to serve as reservoirs for ebola viruses. Similar efforts have been used to predict reservoirs of SARS-CoV-2[14], orthopoxviruses[15], betacoronaviruses[12], Nipah virus[16], and filoviruses outside of equatorial Africa[17]. Thus, we now have tools in place to generate hypotheses for which species are likely to be reservoirs of any particular pathogen species.

Even with hypotheses for which species are likely to serve as a reservoirs in hand, testing and confirming that any individual species serves as an important reservoir remains a significant challenge[12,18–20]. Beyond the obvious complexities and logistical challenges associated with sampling wild animals in remote locations, verifying that an animal is a reservoir requires capturing an animal with a detectable active infection[1]. Prevalence of some zoonotic pathogens is sufficiently high that screening reservoir animals for active shedding is straightforward (e.g., Lassa virus in *Mastomys natalensis*[21]), but more often it is extremely challenging for pathogens that generate short-lived acute infections concentrated at only certain times of the year see[22–26]. In these cases, achieving even a modest chance of capturing an animal with a detectable active infection requires intensive

and temporally focused sampling during periods of peak prevalence[18]. To address different aspects of this problem, several Bayesian approaches have been developed using serosurveillance data to predict incidence and prevalence in reservoir populations. For example, Borremans et al.[27] used information about multiple antibodies over time, pathogen presence, and demographic information to back-calculate the time since infection for individuals to estimate incidence of Morogoro virus infection in multimammate mice (*M. natalensis*). Using a different approach, Pleydell et al.[28] fit an age-structured epidemiological model specific to Ebola virus in straw-colored fruit bats (*Eidolon helvum*) to estimate the timing of peak prevalence in the adult population. Although these methods are robust, adapting them quickly to other systems would be laborious and not always feasible depending on data availability. Thus, a flexible method more easily tailored to different species that requires minimal data would aid empiricists developing surveillance sampling designs to target zoonotic pathogens.

Here we develop a general methodology that can be used to focus reservoir surveillance on periods of time that are most likely to coincide with peak prevalence of a zoonotic pathogen (most often viral pathogens). Our method requires routine serosurveillance data, knowledge of the rate at which detectable antibodies wane, and the rate at which individuals recover from infection. We test the accuracy and utility of our methodology using simulated data and then apply it to systems with real-world importance, Ebola virus (EBOV; *Zaire ebolavirus*) in straw-colored fruit bats (*Eidolon helvum*) and hammer-headed bats (*Hypsignathus monstrosus*) using previously published data. We believe this method is simple enough for wide-reaching application to many field studies. Therefore our method provides a useful tool to guide the planning of field sampling and to study epidemiological dynamics in reservoir populations when data on active infections are rare or absent.

METHODS

Mathematical foundation

Our approach to optimizing surveillance for zoonotic pathogens from serological surveillance data builds from a mathematical model describing the ecology of the reservoir animal and the epidemiology of the pathogen. We illustrate our approach using a model of a reservoir animal that reproduces seasonally and experiences both density independent and density dependent mortality. We assume the pathogen can be adequately described by a modified SIR framework that takes into account both short-term antibody mediated immunity and long-term immunity mediated by a T-cell response. This distinction is important because we assume only the short-term antibody based response is detected by serology[29]. If we further assume individuals encounter one another at random, the ecology and epidemiology of the system can be described using the following system of differential equations:

$$\dot{S} = b(t)N - \beta SI - S\big(\mu + kN\big) + \omega_T R_T \tag{1a}$$

$$\dot{I} = \beta SI - \gamma I - I\big(\mu + kN\big) \tag{1b}$$

$$\dot{R_A} = \gamma I - R_A\big(\mu + kN + \omega_A\big) \tag{1c}$$

$$\dot{R_T} = \omega_A R_A - R_T\big(\mu + kN + \omega_T\big), \tag{1d}$$

where S is the number of susceptible individuals, I is the number of pathogen infected individuals, R_A is the number of individuals with antibodies detectable through serology, R_T is the number of individuals that are immune to pathogen but lack detectable antibodies, and $N = S + I + R_A + R_T$ is the total population size of the reservoir. All model parameters and their biological interpretations are described in table (1).

Table 1: Model parameters and their biological interpretations. All rates are in days unless specified otherwise.

Parameter	Biological interpretation
$b(t)$	Seasonally fluctuating birth rate
μ	Density independent death rate
k	Density dependent death rate
β	Transmission rate
γ	Rate of recovery from infection
ω_A	Rate at which antibodies decay
ω_T	Rate at which T-cell immunity decays

If data on the abundance of each class are available, we could proceed directly from model (1). Unfortunately, this will not generally be the case, and data will more frequently come from serological testing of a random sample of n reservoir animals at various points in time. To calculate the probability that x animals will be seropositive within each sample of size n requires that we make a change of variables (supplemental material, appendix 1) to express model (1) in terms of proportions:

$$\dot{s} = b(t) - s\big(b(t) - \iota\beta N\big) + \omega_T r_T \tag{2a}$$

$$\dot{\iota} = \iota\big(s\beta N - b(t) - \gamma\big) \tag{2b}$$

$$\dot{r}_A = \gamma\iota - r_A\big(\omega_A + b(t)\big) \tag{2c}$$

$$\dot{r}_T = r_A\omega_A - r_T\big(\omega_T + b(t)\big), \tag{2d}$$

where s, ι, r_A, and r_T are the proportion of reservoir animals in each class and N is the total population size of the reservoir animal. With the model now written in terms of proportions, we can proceed to solve for the proportion of animals in the actively infectious class, ι, as a function of the proportion of animals that carry antibodies, $r_A(t)$, using equation (2c):

$$\hat{\iota}(t) = \frac{\dot{r}_A(t) + r_A(t)\big(\omega_A + b(t)\big)}{\gamma}, \tag{3}$$

where $\hat{\iota}(t)$ is the predicted proportion of the population that is actively infected at time t.

Equation (3) demonstrates that we can predict the proportion of the population that is actively infected at any point in time if we can estimate four quantities: 1) the rate at which antibodies are produced following infection, γ; 2) the rate at which antibodies wane over time, ω_A; 3) a function describing the reservoir birth rate over time, $b(t)$; and 4) a function describing seroprevalence over time, $r_A(t)$. We assume that the temporally constant parameters γ and ω_A are known or can be estimated using experimental infections in the lab. In contrast, the seasonal pattern of birth $b(t)$ will generally not be known and may need to be estimated in some cases (supplemental material, appendix 2). If, however, animals live much longer than the lifespan of antibodies such that $b(t) << \omega_A$, birth can be safely ignored to a good approximation (figure S1). Finally, we assume that the seasonal pattern of seroprevalence, $r_A(t)$, will generally be unknown and will need to be estimated from serosurveys. In the next section, we outline how this can be accomplished using routinely collected serological data. All mathematical analyses were performed in Wolfram Mathematica 13.1 [30].

Fitting the mathematical model to data

Estimating a function that describes seasonal patterns of seroprevalence, $\hat{r}_A(t)$, is central to our approach and leverages data that is routinely collected across a wide range of systems. In general, we assume a sample of reservoir animals is captured at

multiple times each year and tested for the presence of antibodies for a target pathogen to give the number of seropositive animals in a sample. Thus, data will consist of a sampling date (t), a sample size (n), and the number of animals within the sample that are seropositive (x). We take two approaches to fitting $\hat{r}_A(t)$, with the best approach largely dependent on the temporal resolution of the data.

Interpolation of temporally rich seroprevalence data

If high-resolution seroprevalence data (e.g., weekly or monthly sampling) are available for a potential reservoir species, interpolation provides an efficient method for fitting the function $r_A(t)$ to the data. We illustrate this approach by applying a kernel smoother to estimate the function, $\hat{r}_A(t)$. Specifically, we use the NadarayaWatson kernel regression estimate available in R[31] with a normal density as the smoothing kernel and a bandwidth of 90. The bandwidth must be increased in cases when data is sparse, thus we used the lowest value possible that accommodated our all of our simulations (see simulated surveillance data section below). We then calculate the derivative of the interpolated function, $\dot{r}_A(t)$, by differencing the fitted values for $\hat{r}_A(t)$ per unit time (e.g. days, weeks, months etc.). As long as parameters γ and ω_A have been estimated independently, and $b(t)$ is negligible (or estimated), this provides the information required for the frequency of infected individuals over time, $\hat{\imath}(t)$ to be predicted using equation (3). Although computationally efficient and conceptually straightforward, we anticipate that this method will not perform well when data are sparse or highly clustered (i.e., when sampling effort is concentrated at specific times of year).

Model fitting for sparse seroprevalence data

In cases when sampling is sporadic and seroprevalence data are sparse, interpolation may not be feasible and an approach based on model-fitting may perform better. This approach uses an understanding of system specific biology to define a mathematical function describing how seroprevalence is expected to change over time. The limited seroprevalence data is then used to estimate the parameters that fine-tune the function $\hat{r}_A(t)$ (e.g., the timing of peaks). Here, we illustrate this approach for systems where seasonal birth pulses are thought to cause fluctuations in the prevalence of infection and concomitant fluctuations in seroprevalence.

In systems where seasonal birth pulses occur, we expect, in general, a subsequent increase in infected individuals followed by a downstream increase in individuals that have seroconverted. Qualitatively, this expectation can be modeled using a modified periodic Gaussian function e.g.,[32]:

$$r_A^*(t) = C_2 - C_1 \cdot e^{-a\cos^2(\pi f t - \phi)}. \tag{4}$$

Here $r_A^*(t)$ is a function specifying the predicted proportion of seropositive animals at time t, C_2 adjusts the average value of seroprevalence over time, C_1 sets the amplitude of seasonal fluctuations in seroprevalence, a controls the shape of seasonal fluctuations, ϕ defines the phase shift, and f specifies the frequency. We assume f is determined by the natural history of the reservoir species and is known. For example, a reservoir species that reproduces either once or twice per year in a regular pattern would have values of $f = 1/365$ and $f = 2/365$, respectively, if the time units are given in days. In contrast, we expect C_1, C_2, a, and ϕ to be unknown and require estimation.

We used Bayesian inference to estimate the unknown parameters in equation (4) and estimate the uncertainty in our estimates for $\hat{\imath}_{peak}$ using 95% credible intervals (CI). Specifically, the likelihood of observing a temporal sequence of seroprevalence values is:

$$\mathcal{L}(\theta) = \prod_{i=1}^{\tau} \binom{n_i}{x_i} r_A^*(t_i)^{x_i} \left(1 - r_A^*(t_i)\right)^{n_i - x_i}, \tag{5}$$

where the product is carried over τ total sampling time points and $\theta = \{C_1, C_2, a, \phi\}'$. For each time point i, n_i defines the number of animals sampled at time point i, x_i defines the number of sampled animals found to be seropositive at time point i, and

t_i defines the time at which sample i was collected. Prior distributions for model parameters and details of the Bayesian estimation procedure are given in supplemental material, appendix 3. Bayesian estimation was performed using rstan[33].

Simulating surveillance data

To determine if our methods accurately predict the true peak prevalence of infection, ι_{peak}, we applied each method to simulated data sets. Specifically, we simulated a pathogen circulating in a wild animal population using model (1) with semi-annual birth pulses using equation (S6). In general, this leads to two peaks in prevalence and seroprevalence each year, a pattern observed in many bat species e.g.,[34–36]. Simulations focused on three different scenarios: low, medium, or high amplitude cycles in seroprevalence, $r_A(t)$, and prevalence, $\iota(t)$, with the specific parameter values used provided in table (S2). We generated 100 replicate stochastic simulations for each scenario using the Gillespie algorithm with a tau leaping approximation[37]. Simulations were initiated at the endemic disease equilibrium (supplemental material, appendix 1) and run for 10 years. We used the last 394 days for analyses to include peaks occurring at the end of year 9 to beginning of year 10, and all days in year 10. The two predicted peaks within the final 394 days, $\hat{\iota}_{peak}$, were determined for each simulated data set by finding the time point associated with the maximum value between days [0,170] and the time point associated with the maximum value between days [170,360].

We applied our methodology to the simulated data for a range of possible field sampling designs. First, we analyzed the simulated data sets assuming field sampling was performed at evenly spaced time intervals (daily, weekly, bi-weekly, monthly, bi-monthly) over the 394 day study period. Second, we analyzed the simulated data sets assuming the number of sampling days was fixed at 42 days, but the distribution of these days over the year differed (evenly spaced days, random days, 3-day clusters, 7-day clusters). Each of the nine sampling designs was applied to the low, medium, and high amplitude seroprevalence cycle scenarios to yield 27 different combinations of epidemiological dynamics and sampling schemes (table S3). For each day of sampling, we assumed $n = 20$ animals were captured at random and tested for antibodies to the focal pathogen to yield an estimate for seroprevalence.

To evaluate the performance of our method, we compared the probability of detecting an actively infected animal (e.g., through PCR, culture, or sequencing) when sampling was timed using our method with two benchmarks: 1) the best case scenario where sampling was performed at the true peak and 2) the null solution where sampling was performed on a random day. In each case, a sample of 20 animals was drawn at random and the number that were actively infected was recorded. Sampling was repeated ten times for each case and the probability of detecting an actively infected animal calculated as the number of trials in which at least one infected animal was found. Details on all simulations are given in supplemental material, appendix 4. All simulations were performed in R[31].

Study Populations and Surveillance Sampling

African fruit bats are likely candidate reservoir hosts for Ebolaviruses evidenced by the presence of antibodies in many species and viral RNA sequenced from several species, yet no replicating viral strain has been isolated from a wild bat population despite extensive field sampling see[22–25]. Many bat species have highly synchronous birth cycles[34] that can translate into cycles of infection prevalence[32]. In addition, Ebolaviruses are cleared by their hosts and therefore viral shedding may only be detected during a brief window[38]. Thus, predicting transmission cycles of Ebolaviruses in putative reservoir hosts would help to optimize surveillance sampling and to understand spillover and the origins of Ebola virus disease in humans.

Two examples of frugivorious bat species with medium to high seroprevalence and the hypothesized potential to cause Ebolavirus spillover events are straw-colored fruit bats (*Eidolon helvum*) and hammer-headed bats (*Hypsignathus monstrosus*)[38–40]. *E. helvum* are commmon fruit bats that form large seasonal aggregations[38] and reproduce annually[41]. *H. monstrosus* form large breeding aggregations[42], but unlike *E. helvum*, reproduce semi-annually[41]. Djomsi et al.[38] captured free-ranging bats from a roosting site in Yaounde, Cameroon, and at a feeding site 40 km away near Obala, Cameroon. Samples were collected at approximately monthly intervals between December 2018 and November 2019, with the largest inter-sampling interval span-

ning two months. Whole blood samples and rectal and oral swabs preserved in RNA-later were collected from individual bats. Bat species, *E. helvum* and *H. monstrosus*, were identified by molecular testing. Djomsi et al.[38] screened *E. helvum* and *H. monstrosus* samples for antibodies to three *Ebolavirus* species using a Luminex-based serological assay previously adapted for bats see[38]. They also tested for active infections in *E. helvum* using a semi-nested PCR assay specific to Ebola virus (EBOV; *Zaire ebolavirus*) targeting a 184 bp fragment on the VP35 gene see[38]. For analyses in this study, we used the results from the Res1GP.ZEBVkiss antigenic test, a test for on the glycoprotein of EBOV, following[28]. Specific details of all methods and data are publicly available from[38] and[28].

To parameterize our models for *E. helvum* and *H. monstrosus*, we used values previously estimated values for the recovery rate and rate of waning antibodies. Pleydell et al.[28] estimated the recovery rate ($\gamma = 1/1.5$ weeks) and rate of waning antibodies ($\omega_A = 1/75$ weeks) for the *E. helvum* population in Cameroon, but did not estimate these value for *H. monstrosus*. For *H. monstrosus*, we used measurements from experimental studies in Egyptian fruit bats (*Rousettus aegyptiacus*) with Marburg virus (MARV; *Marburg marburgvirus*) to approximate parameter values for the recovery rate ($\gamma = 1/1.43$ weeks)[43] and the rate of waning antibodies ($\omega_A = 1/12.9$ weeks)[44].

RESULTS

Optimizing surveillance on simulated data

Interpolation of temporally rich seroprevalence data

We begin our analyses by testing our methods on simulated surveillance data. Figure 1 shows an example of the true population curves for $r_A(t)$ and $\iota(t)$ and the estimated curves, $\hat{r}_A(t)$ and $\hat{\iota}(t)$, that were fitted to simulated serological data using interpolation. We find that we can successfully estimate $\hat{r}_A(t)$ and predict prevalence pulses in populations with different epidemiological dynamics (e.g., low, medium, and high amplitude dynamics in figure 1) using interpolation. When surveillance sampling occurs at sufficient frequency and at even intervals across time, interpolation provides a good approximation to the true epidemiological dynamics such that surveillance sampling can be optimized to detect active infections (figures 2 and 3a). The accuracy of the predictions for the timing of peak prevalence in the population from interpolation for all sampling schemes are given in table (S4). When the data requirements are met, this method can also be used retrospectively to understand epidemiological dynamics when episodic shedding occurs randomly, for example, not necessarily coinciding with seasonal birth pulses (figure S7). However, interpolation methods do not accurately predict the peak timing if serology data is sparse or sampling is highly clustered in time (see figures 2 and 3a). In these cases, model fitting is a better option.

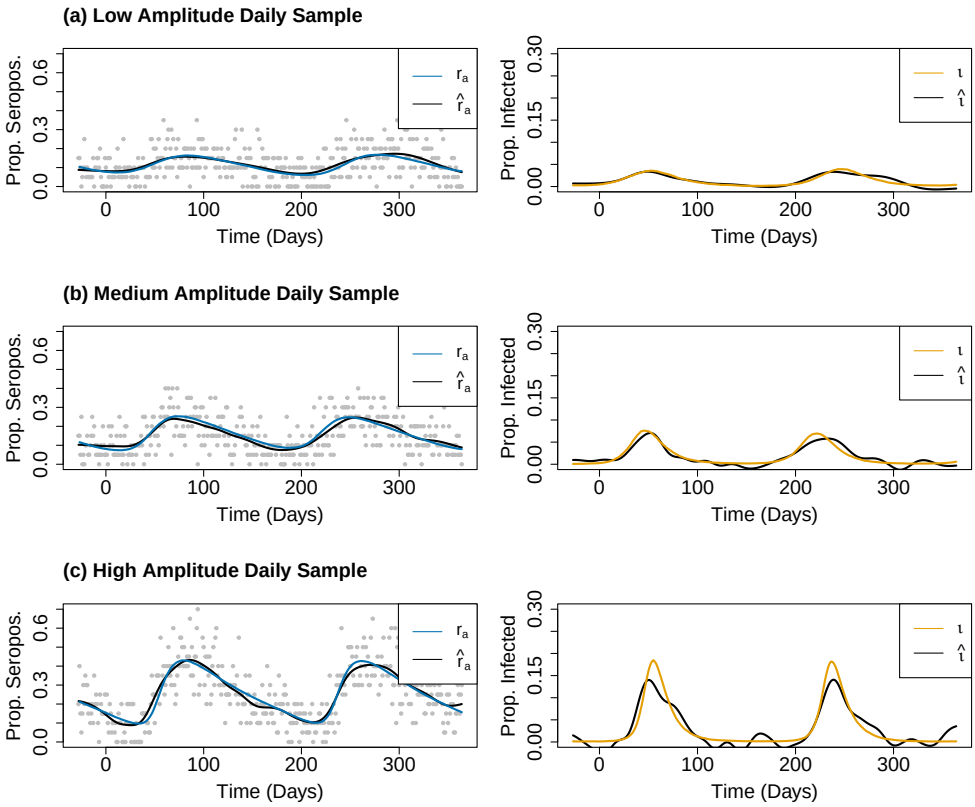

Figure 1: Results from interpolating serological data sampled daily for (a) low, (b) medium, and (c) high amplitude epidemic curves. Grey points represent the raw simulated data.

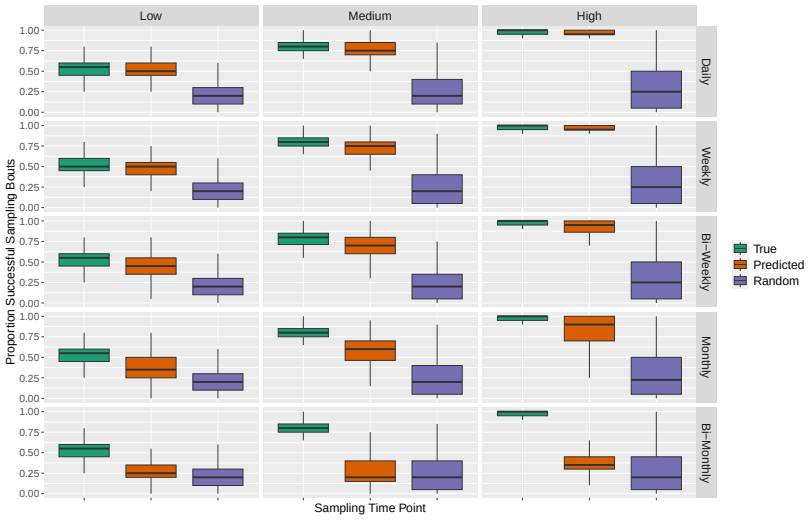

Figure 2: Proportion successful sampling bouts that occurred when the simulated population was sampled during the true peaks, ι_{peak}, the interpolation prediction of peaks, $\hat{\iota}_{peak}$, and a random time point. The proportion of successful sampling bouts are shown for three different types of disease dynamics, where the amplitude of the cycles is low, medium, and high, and for five different sampling schemes, when sampling occurs daily, weekly, bi-weekly, monthly, and bi-monthly over 394 days.

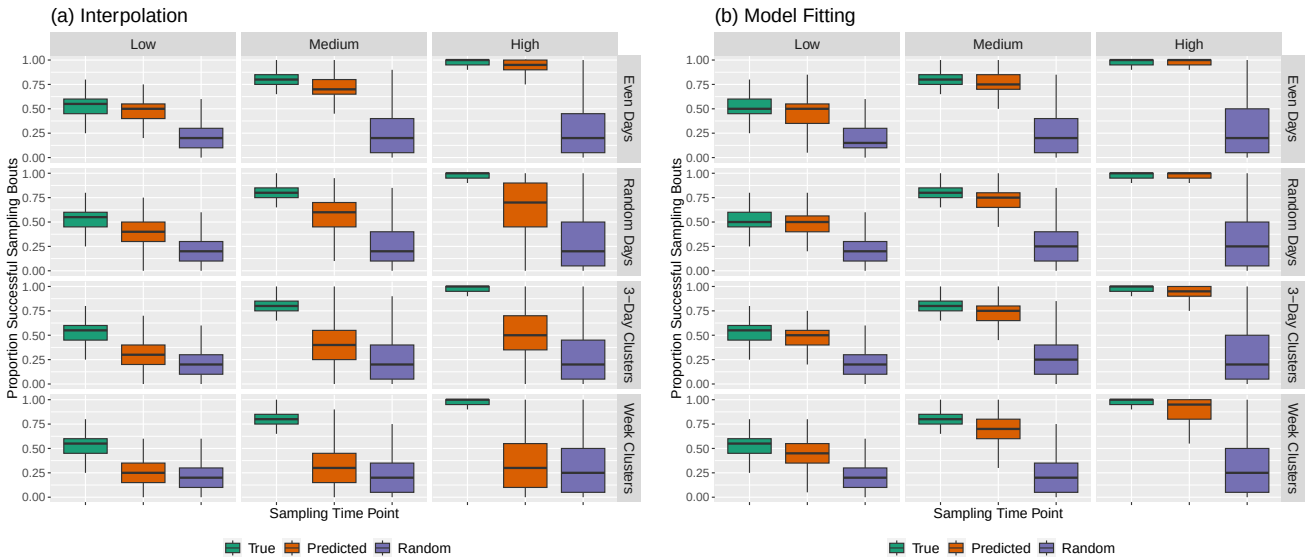

Figure 3: Proportion successful sampling bouts that occurred when the simulated population was sampled during the true peaks, ι_{peak}, the predicted peaks, $\hat{\iota}_{peak}$, and a random time point when the predictions for $\hat{r}_A(t)$ were made by (a) interpolation or (b) model fitting. The proportion of successful sampling bouts are shown for three different types of disease dynamics, where the amplitude of the cycles is low, medium, and high, and for four different 42-day sampling schemes, when sampling occurs at even intervals, random days, 3-day clusters, and week clusters.

Model fitting for sparse seroprevalence data

Although estimating the function $\hat{r}_A(t)$ using model fitting is more computationally intensive than interpolation, our results show that this approach can accurately predict the timing of peak prevalence when interpolation would fail (figure 3a). Specifically, as seroprevalence data becomes less evenly distributed, we find that the model fitting approach continues to provide accurate guidance for sampling whereas the guidance provided by the interpolation approach degrades (figure 3b and 4). The accuracy of the predictions for the timing of peak viral shedding in the population from $r^*_A(t)$, the size of the 95% CI estimated via Bayesian inference, and the proportion of times the true population peak falls within the CIs are summarized in table (S5).

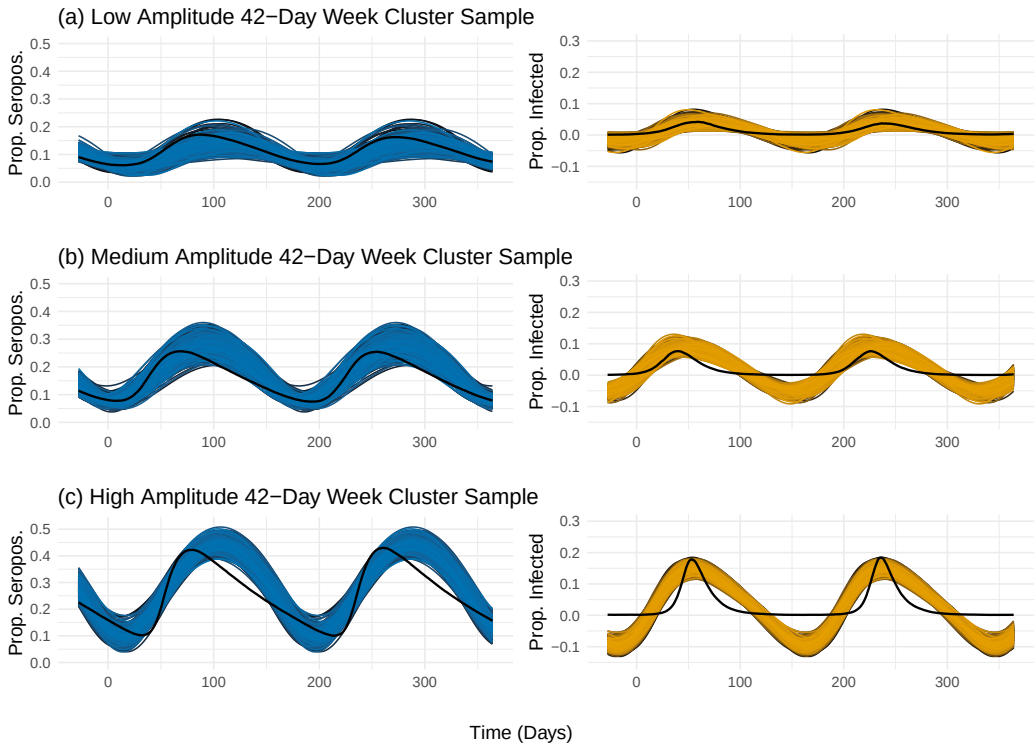

Figure 4: Results from model fitting with 42-day weekly clustered simulated serosurveillance data from (a) low, (b) medium, and (c) high amplitude epidemic curves. The blue and yellow lines represent the distribution of curves falling within the 95% CIs after Bayesian parameter estimation of $r_A^*(t)$ and predicting $\hat{\imath}(t)$, respectively. The black lines represent the true population simulated dynamics.

Application to putative Ebolavirus reservoirs

In Cameroon, the fruit bat species *E. helvum* and *H. monstrosus* were shown to carry antibodies against EBOV but no active infections were detected in *E. helvum*[38]. Djomsi et al.[38] did not test the *H. monstrosus* population for active infections, however, *H. monstrosus* is one of three bat species for which EBOV has been detected by real-time PCR and partially sequenced[45].

We used publicly available data from[28] to predict the peak period of active infection, $\hat{\imath}_{peak}$, using our methodology. This data set includes seroprevalence and the proportion of animals lactating for each species. First, we tested the assumption that *E. helvum* reproduces annually and *H. monstrosus* reproduces semi-annually. Figures (S3) and (S5) demonstrate one annual birth pulse for *E. helvum* and two annual birth pulses for *H. monstrosus*, respectively. Next, we used results from serosurveys to predict annual viral pulses, $\hat{\imath}_{peaks}$, in *E. helvum* by fitting the data to $r_A^*(t)$ for EBOV (figure 5). Figure (S4) shows the estimated serodynamics and predicted infection prevalence for this population. These results suggest this population has a high amplitude cycle relative to our simulated data, with an average amplitude of 0.56 an 95% CI equal to [0.51, 0.62], meaning that sampling this population at peak prevalence greatly optimizes sampling for active infections. The distribution of the timing of predicted peaks is given in figure (5) with the mode occurring at week 32 and 95% CI spanning weeks [31,33]. No samples contained in this dataset were collected during this predicted window of peak prevalence[28].

We used the same methodology to predict the period of peak prevalence for *H. monstrosus*. The estimated temporal patterns of seroprevalence and prevalence for this population are shown in figure (S6). These results suggest that this population has a low amplitude cycle, with an average amplitude of 0.053 and a 95% CI equal to [0.00, 0.14]. The estimates and 95% CIs for the two peaks are the first mode occurring on week 27 within the interval [20.00, 32.00] and the second mode occurring on week 1 within the interval [46.00, 6.00] (weeks within a year are counted from from 0 to 51) (figure 6). Djomsi et al.[38] collected samples for this species during the predicted peak intervals, but the samples were not tested for active infections of EBOV.

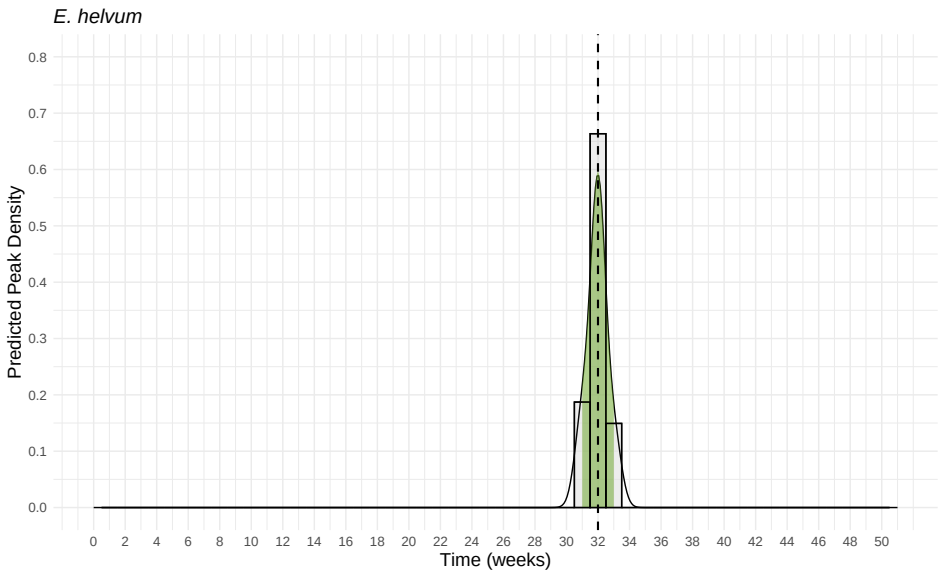

Figure 5: Distribution of weeks where the annual peak viral pulse was predicted for *E. helvum*. The vertical dashed line represents the mode and the green shaded area represents the 95% CI.

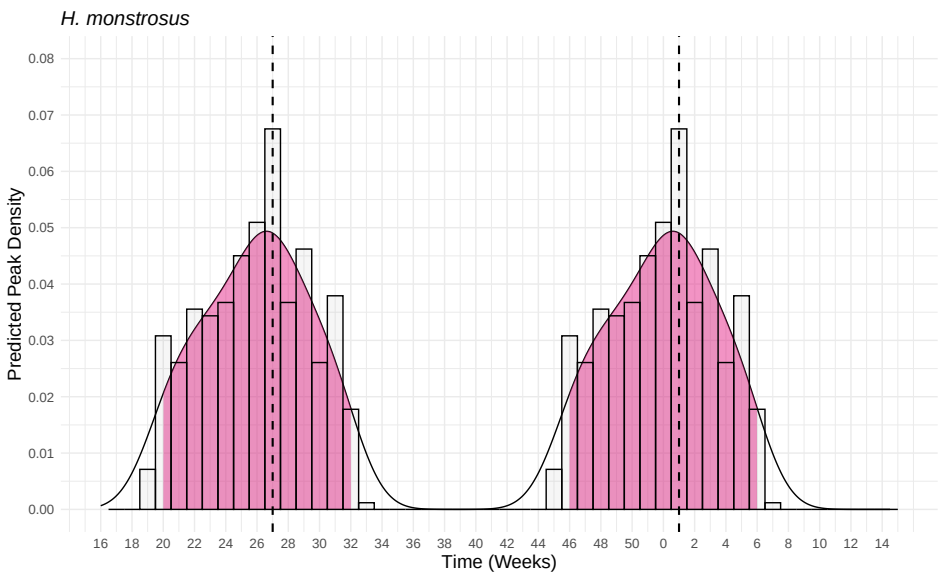

Figure 6: Distribution of weeks where the semi-annual peak viral pulses were predicted for *H. monstrosus*. The vertical dashed lines represent the modes and the pink shaded areas represent the 95% CIs for each pulse. Note the timescale on the x-axis begins at week 16 to accommodate the second peak that occurs at the end/beginning of each year.

DISCUSSION

We have developed a general methodology for predicting the timing of peak pathogen prevalence in seasonally fluctuating wildlife populations using temporally structured serological data. Our approach is motivated by the possibility that successful sampling of actively infected reservoir animals has been impeded by seasonal fluctuations in pathogen prevalence driven by seasonal birth cycles. By focusing the search for active infections on specific periods of time where infections are most likely to be discovered, our method may facilitate confirmation of long-suspected reservoir hosts. Thus, our method leverages routinely collected serosurveillance data to extract information about the temporal pattern of active infection. When serosurveillance data is sufficiently rich for the temporal pattern of seroprevalence to be interpolated, our method is particularly straightforward, computationally inexpensive, and accurate. Even when serosurveillance data is temporally sparse, however, our method can be

used to generate accurate predictions by first fitting a mathematical model to the serological data. This latter approach, however, is more computationally intensive and requires an additional assumption about the timing of the birth cycle.

Applying our methodology to two bat species in Cameroon, *E. helvum* and *H. monstrosus*[38], long hypothesized to harbor EBOV, demonstrates its utility. Our results suggest the population of *E. helvum* has one prevalence peak occurring between weeks 31-33 each year. The population of *H. monstrosus* has much wider semi-annual peak intervals spanning weeks 20 to 32 and 46 to 6 in the following year. If accurate, these interval estimates can be used to plan future surveillance surveys or predict periods when a high proportion of infected animals may pose an increased threat of zoonotic spillover. Unfortunately, validating our predictions will only be possible when animals with active infections have been captured from these populations. Nonetheless, evidence exists to support our interval estimates for each species. Our peak interval for *E. helvum* corresponds to the interval (weeks 30-31) predicted by Pleydell et al.[28] who estimated an age-structured model to obtain the highest probability predicted annual peak in the density of infectious adults. The semi-annual *H. monstrosus* intervals overlap the weeks in 2003 (week 5 and 22) in which Leroy et al.[45] captured bats PCR-positive for EBOV on the border between Gabon and the Republic of the Congo.

Although we demonstrate with simulate data our methodology can generate robust predictions for the timing of peak prevalence in reservoir populations, limitations of our model may still exist. First, the simulation testing assumed that the mathematical model underlying our method accurately reflected the true biological processes. If the assumptions of our relatively simple compartment model are violated in the wild, our testing may overestimate the performance of our method. For instance, the model we have studied here ignores age structure which may have a significant impact on the relationship between seroprevalence and prevalence if sampling is not random with respect to age class e.g.,[28,34]. The method we present here also assumes seasonality is driven by fluctuations in birth rate rather than seasonal changes in animal behavior that may influence contact rates and transmission e.g.,[42]. Even though we did not study these alternative scenarios directly, instead choosing to focus on a simple but general scenario, it will often be possible to integrate alternative biological assumptions by simply exchanging the underlying mechanistic model.

Next, a potential limitation specific to our model fitting method is that we assume the epidemiological cycles occur consistently over time and the frequency can be specified using the number of birth pulses that occur annually for a particular species. In reality, prevalence pulses can occur stochastically e.g.,[46,47], annual patterns in some population include skip years e.g.,[28,48] or episodic shedding can be hard to distinguish from transient epidemics[49]. If epidemiological cycles cannot be approximated by a regular pattern, our model fitting method would not be appropriate. Our method also requires the rate of waning antibodies to either be known or estimated independently. Thus, our predicted peak intervals from model fitting are conditioned on specific values for rate of waning antibodies. If including uncertainty for these estimates is desired, our likelihood framework used in model fitting would easily accommodate a distribution for the rate of waning antibodies.

Last, our general method requires binary data describing whether an animal is seropositive or seronegative. Serological data is prone to cross-reactivity[50] resulting in low specificity and variable sensitivity dependent on the immune dynamics of the target species and pathogen, secondary antibody selection[51], and method of pathogen inactivation[52]. We assume reliable thresholds will be used to determine seropositivity, but we do not provide a method to include the uncertainty from serological data in our model.

Even in the face of these challenges, pathogen surveillance in wild animal populations is essential for identifying reservoir species, collecting pathogen samples for genetic characterization, and predicting when spillover is most likely to occur. By leveraging routinely collected serosurveys to optimize pathogen surveillance, the methodology we develop here has the potential to reduce the cost and labor associated with pathogen surveillance and increase our ability to successfully sample pathogens that reach appreciable prevalence at only specific times of year. More broadly, this methodology can be used to identify times of year when pathogen prevalence should peak, providing guidance for interventions aimed at reducing spillover risk.

ACKNOWLEDGMENTS

Funding was provided by the Centre for Research in Emerging Infectious Diseases - East and Central Africa (CREID-ECA) grant number U01AI151799 in support of EC and SNS, PIPP Phase I: Predicting Emergence in Multidisciplinary Pandemic Tipping-points (PREEMPT) from the U.S. National Science Foundation (NSF) grant number 2200140 in support of EC, Verena (virale-mergence.org) from NSF including NSF BII 2021909 and NSF BII 2213854 and the US National Institute of Allergy and Infectious Disease/National Institutes of Health (NIAID/NIH) grant number U01AI151799 in support of SNS, NIH 2R01GM122079-05A1 awarded to SNL and NSF DEB 2314616 awarded to SNL.

DATA AVAILABILITY

All data used in this study was previously published and can be found online at at https://doi.org/10.5281/zenodo.8193102 from [28]. The data, R code and Mathematica Notebook used in this study can be found online at https://github.com/erinclancey/STOPPP-Model.

AUTHOR COMPETING INTERESTS

All authors declare we have no competing interests.

REFERENCES

[1] Raina K Plowright, Colin R Parrish, Hamish McCallum, Peter J Hudson, Albert I Ko, Andrea L Graham, and James O Lloyd-Smith. Pathways to zoonotic spillover. *Nature Reviews Microbiology*, 15(8):502–510, 2017.
[2] Colin J Carlson, Maxwell J Farrell, Zoe Grange, Barbara A Han, Nardus Mollentze, Alexandra L Phelan, Angela L Rasmussen, Gregory F Albery, Bernard Bett, David M Brett-Major, et al. The future of zoonotic risk prediction. *Philosophical Transactions of the Royal Society B*, 376(1837):20200358, 2021.
[3] Edward C Holmes. The ecology of viral emergence. *Annual Review of Virology*, 9:173–192, 2022.
[4] Edward C Holmes, Andrew Rambaut, and Kristian G Andersen. Pandemics: spend on surveillance, not prediction. *Nature*, 558(7709):180–182, 2018.
[5] Stephen S Morse, Jonna AK Mazet, Mark Woolhouse, Colin R Parrish, Dennis Carroll, William B Karesh, Carlos Zambrana-Torrelio, W Ian Lipkin, and Peter Daszak. Prediction and prevention of the next pandemic zoonosis. *The Lancet*, 380(9857):1956–1965, 2012.
[6] Jamie K Reaser, Arne Witt, Gary M Tabor, Peter J Hudson, and Raina K Plowright. Ecological countermeasures for preventing zoonotic disease outbreaks: when ecological restoration is a human health imperative. *Restoration Ecology*, 29(4):e13357, 2021.
[7] Susanne H Sokolow, Nicole Nova, Kim M Pepin, Alison J Peel, Juliet RC Pulliam, Kezia Manlove, Paul C Cross, Daniel J Becker, Raina K Plowright, Hamish McCallum, et al. Ecological interventions to prevent and manage zoonotic pathogen spillover. *Philosophical Transactions of the Royal Society B*, 374(1782):20180342, 2019.
[8] Salah Uddin Khan, Emily S Gurley, M Jahangir Hossain, Nazmun Nahar, MA Yushuf Sharker, and Stephen P Luby. A randomized controlled trial of interventions to impede date palm sap contamination by bats to prevent nipah virus transmission in bangladesh. *PLoS ONE*, 7(8):e42689, 2012.
[9] Stephanie Martinez, Ava Sullivan, Emily Hagan, Jonathan Goley, Jonathan H Epstein, Kevin J Olival, Karen Saylors, Jason Euren, James Bangura, Sijali Zikankuba, et al. Living safely with bats: Lessons in developing and sharing a global one health educational resource. *Global Health: Science and Practice*, 10(6), 2022.
[10] Scott L Nuismer and James J Bull. Self-disseminating vaccines to suppress zoonoses. *Nature ecology & evolution*, 4(9):1168–1173, 2020.
[11] Megan E Griffiths, Diana K Meza, Daniel T Haydon, and Daniel G Streicker. Inferring the disruption of rabies circulation in vampire bat populations using a betaherpesvirus-vectored transmissible vaccine. *Proceedings of the National Academy of Sciences*, 120(11):e2216667120, 2023.
[12] Daniel J Becker, Gregory F Albery, Anna R Sjodin, Timothée Poisot, Laura M Bergner, Binqi Chen, Lily E Cohen, Tad A Dallas, Evan A Eskew, Anna C Fagre, et al. Optimising predictive models to prioritise viral discovery in zoonotic reservoirs. *The Lancet Microbe*, 3(8):e625–e637, 2022.
[13] John Paul Schmidt, Sean Maher, John M Drake, Tao Huang, Maxwell J Farrell, and Barbara A Han. Ecological indicators of mammal exposure to ebolavirus. *Philosophical Transactions of the Royal Society B*, 374(1782):20180337, 2019.
[14] Ilya R Fischhoff, Adrian A Castellanos, João PGLM Rodrigues, Arvind Varsani, and Barbara A Han. Predicting the zoonotic capacity of mammals to transmit sars-cov-2. *Proceedings of the Royal Society B*, 288(1963):20211651, 2021.
[15] Katie K Tseng, Heather Koehler, Daniel J Becker, Rory Gibb, Colin J Carlson, Maria del Pilar Fernandez, and Stephanie N Seifert. Viral genomic features predict orthopoxvirus reservoir hosts. *bioRxiv*, 2023.
[16] Raina K Plowright, Daniel J Becker, Daniel E Crowley, Alex D Washburne, Tao Huang, PO Nameer, Emily S Gurley, and Barbara A Han. Prioritizing surveillance of nipah virus in india. *PLoS neglected tropical diseases*, 13(6):e0007393, 2019.
[17] Barbara A Han, John Paul Schmidt, Laura W Alexander, Sarah E Bowden, David TS Hayman, and John M Drake. Undiscovered bat hosts of filoviruses. *PLoS neglected tropical diseases*, 10(7):e0004815, 2016.
[18] Raina K Plowright, Daniel J Becker, Hamish McCallum, and Kezia R Manlove. Sampling to elucidate the dynamics of infections in reservoir hosts. *Philosophical Transactions of the Royal Society B*, 374(1782):20180336, 2019.
[19] Cara E Brook, Hafaliana C Ranaivoson, Christopher C Broder, Andrew A Cunningham, Jean-Michel Héraud, Alison J Peel, Louise Gibson, James LN Wood, C Jessica Metcalf, and Andrew P Dobson. Disentangling serology to elucidate henipa-and filovirus transmission in madagascar fruit bats. *Journal of Animal Ecology*, 88(7):1001–1016, 2019.
[20] Amy T Gilbert, AR Fooks, DTS Hayman, DL Horton, T Müller, R Plowright, AJ Peel, R Bowen, JLN Wood, J Mills, et al. Deciphering serology to understand the ecology of infectious diseases in wildlife. *EcoHealth*, 10:298–313, 2013.
[21] Elisabeth Fichet-Calvet, Emilie Lecompte, Lamine Koivogui, Barré Soropogui, Amadou Doré, Fodé Kourouma, Oumar Sylla, Stéphane Daffis, Kékoura Koulémou, and Jan Ter Meulen. Fluctuation of abundance and lassa virus prevalence in mastomys natalensis in guinea, west africa. *Vector-Borne and Zoonotic Diseases*, 7(2):119–128, 2007.
[22] Alexandre Caron, Mathieu Bourgarel, Julien Cappelle, Florian Liégeois, Hélène M De Nys, and François Roger. Ebola virus maintenance: if not (only) bats, what else? *Viruses*, 10(10):549, 2018.
[23] Lisa K Koch, Sarah Cunze, Judith Kochmann, and Sven Klimpel. Bats as putative zaire ebolavirus reservoir hosts and their habitat suitability in africa. *Scientific reports*, 10(1):14268, 2020.
[24] Siv Aina J Leendertz, Jan F Gogarten, Ariane Düx, Sebastien Calvignac-Spencer, and Fabian H Leendertz. Assessing the evidence supporting fruit bats as the primary reservoirs for ebola viruses. *EcoHealth*, 13:18–25, 2016.
[25] Amy J Schuh, Brian R Amman, and Jonathan S Towner. Filoviruses and bats. *Microbiology Australia*, 38(1):12–16, 2017.
[26] Daniel J Becker, Daniel E Crowley, Alex D Washburne, and Raina K Plowright. Temporal and spatial limitations in global surveillance for bat filoviruses and henipaviruses. *Biology Letters*, 15(12):20190423, 2019.
[27] Benny Borremans, Niel Hens, Philippe Beutels, Herwig Leirs, and Jonas Reijniers. Estimating time of infection using prior serological and individual information can greatly improve incidence estimation of human and wildlife infections. *PLoS computational biology*, 12(5):e1004882, 2016.
[28] David RJ Pleydell, Innocent Ndong Bass, Flaubert Auguste Mba Djondzo, Dowbiss Meta Djomsi, Charles Kouanfack, Martine Peeters, and Julien Cappelle. A bayesian analysis of birth pulse effects on the probability of detecting ebola virus in fruit bats. *bioRxiv*, pages 2023–08, 2023.
[29] Amy J Schuh, Brian R Amman, Tara K Sealy, Jessica R Spengler, Stuart T Nichol, and Jonathan S Towner. Egyptian rousette bats maintain long-term protective immunity against marburg virus infection despite diminished antibody levels. *Scientific reports*, 7(1):8763, 2017.
[30] Wolfram Research, Inc. Mathematica, 2021. Place: Champaign, Illinois.
[31] R Core Team. *R: A Language and Environment for Statistical Computing*. R Foundation for Statistical Computing, Vienna, Austria, 2023.
[32] A. J. Peel, J. R. C. Pulliam, A. D. Luis, R. K. Plowright, T. J. O'Shea, D. T. S. Hayman, J. L. N. Wood, C. T. Webb, and O. Restif. The effect of seasonal birth pulses on pathogen persistence in wild mammal populations. *Proceedings of the Royal Society B: Biological Sciences*, 281(1786):20132962, July 2014.
[33] Stan Development Team. *RStan: the R interface to Stan*, 2023. R package version 2.32.3.
[34] David TS Hayman. Biannual birth pulses allow filoviruses to persist in bat populations. *Proceedings of the Royal Society B: Biological Sciences*, 282(1803):20142591, 2015. Publisher: The Royal Society.
[35] Marinda Mortlock, Marike Geldenhuys, Muriel Dietrich, Jonathan H Epstein, Jacqueline Weyer, Janusz T Pawęska, and Wanda Markotter. Seasonal shedding patterns of diverse henipavirus-related paramyxoviruses in egyptian rousette bats. *Scientific reports*, 11(1):24262, 2021.
[36] C Reed Hranac, Jonathan C Marshall, Ara Monadjem, and David TS Hayman. Predicting ebola virus disease risk and the role of african bat birthing. *Epidemics*, 29:100366, 2019.
[37] Daniel T Gillespie. Approximate accelerated stochastic simulation of chemically reacting systems. *The Journal of chemical physics*, 115(4):1716–1733, 2001.
[38] Dowbiss Meta Djomsi, Flaubert Auguste Mba Djonzo, Innocent Ndong Bass, Maëliss Champagne, Audrey Lacroix, Guillaume Thaurignac, Amandine Esteban, Helene De Nys, Mathieu Bourgarel, Jane-Francis Akoachere, Eric Delaporte, Ahidjo Ayouba, Julien Cappelle, Eitel Mpoudi Ngole, and Martine Peeters. Dynamics of Antibodies to Ebolaviruses in an Eidolon helvum Bat Colony in Cameroon. *Viruses*, 14(3):560, March 2022.

[39] Seth D Judson, Robert Fischer, Andrew Judson, and Vincent J Munster. Ecological contexts of index cases and spillover events of different ebolaviruses. *PLoS pathogens*, 12(8):e1005780, 2016.
[40] RA Kock, M Begovoeva, R Ansumana, and R Suluku. Searching for the source of ebola: the elusive factors driving its spillover into humans during the west african outbreak of 2013–2016. *Rev Sci Tech*, 38(1):113–22, 2019.
[41] Carmen D Soria, Michela Pacifici, Moreno Di Marco, Sarah M Stephen, and Carlo Rondinini. COMBINE: a coalesced mammal database of intrinsic and extrinsic traits. *Ecology*, 102(6):e03344, 2021.
[42] Sarah H Olson, Gerard Bounga, Alain Ondzie, Trent Bushmaker, Stephanie N Seifert, Eeva Kuisma, Dylan W Taylor, Vincent J Munster, and Chris Walzer. Lek-associated movement of a putative ebolavirus reservoir, the hammer-headed fruit bat (hypsignathus monstrosus), in northern republic of congo. *PloS ONE*, 14(10):e0223139, 2019.
[43] Amy J. Schuh, Brian R. Amman, Tara K. Sealy, Jessica R. Spengler, Stuart T. Nichol, and Jonathan S. Towner. Egyptian rousette bats maintain long-term protective immunity against Marburg virus infection despite diminished antibody levels. *Scientific Reports*, 7(1):1–7, 2017. Publisher: Nature Publishing Group.
[44] Brian R. Amman, Megan EB Jones, Tara K. Sealy, Luke S. Uebelhoer, Amy J. Schuh, Brian H. Bird, JoAnn D. Coleman-McCray, Brock E. Martin, Stuart T. Nichol, and Jonathan S. Towner. Oral shedding of Marburg virus in experimentally infected Egyptian fruit bats (Rousettus aegyptiacus). *Journal of wildlife diseases*, 51(1):113–124, 2015.
[45] Eric M Leroy, Brice Kumulungui, Xavier Pourrut, Pierre Rouquet, Alexandre Hassanin, Philippe Yaba, André Délicat, Janusz T Paweska, Jean-Paul Gonzalez, and Robert Swanepoel. Fruit bats as reservoirs of ebola virus. *Nature*, 438(7068):575–576, 2005.
[46] Michael Begon, Sandra Telfer, Matthew J Smith, Sarah Burthe, Steve Paterson, and Xavier Lambin. Seasonal host dynamics drive the timing of recurrent epidemics in a wildlife population. *Proceedings of the Royal Society B: Biological Sciences*, 276(1662):1603–1610, 2009.
[47] Herwig Leirs, Nils Chr Stenseth, James D Nichols, James E Hines, Ron Verhagen, and Walter Verheyen. Stochastic seasonality and nonlinear density-dependent factors regulate population size in an african rodent. *Nature*, 389(6647):176–180, 1997.
[48] Lewi Stone, Ronen Olinky, and Amit Huppert. Seasonal dynamics of recurrent epidemics. *Nature*, 446(7135):533–536, 2007.
[49] Raina K Plowright, Peggy Eby, Peter J Hudson, Ina L Smith, David Westcott, Wayne L Bryden, Deborah Middleton, Peter A Reid, Rosemary A McFarlane, Gerardo Martin, et al. Ecological dynamics of emerging bat virus spillover. *Proceedings of the royal society B: biological sciences*, 282(1798):20142124, 2015.
[50] Amy J Schuh, Brian R Amman, Tara S Sealy, Timothy D Flietstra, Jonathan C Guito, Stuart T Nichol, and Jonathan S Towner. Comparative analysis of serologic cross-reactivity using convalescent sera from filovirus-experimentally infected fruit bats. *Scientific Reports*, 9(1):6707, 2019.
[51] K Nielsen, P Smith, W Yu, P Nicoletti, P Elzer, A Vigliocco, P Silva, R Bermudez, T Renteria, F Moreno, et al. Enzyme immunoassay for the diagnosis of brucellosis: chimeric protein a–protein g as a common enzyme labeled detection reagent for sera for different animal species. *Veterinary microbiology*, 101(2):123–129, 2004.
[52] So Lee Park, Yan-Jang S Huang, Wei-Wen Hsu, Susan M Hettenbach, Stephen Higgs, and Dana L Vanlandingham. Virus-specific thermostability and heat inactivation profiles of alphaviruses. *Journal of Virological Methods*, 234:152–155, 2016.